Supplementary

A

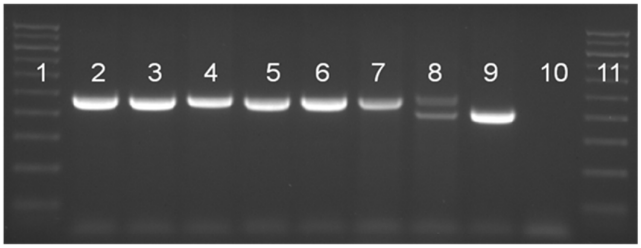

slot	Sample
1	DNA ladder
2	$Col1a1^{Eng-/-}$ mouse
3	$Col1a1^{Eng-/-}$ mouse
4	$Col1a1^{Eng-/-}$ mouse
5	$Col1a1^{Eng-/-}$ mouse
6	$Col1a1^{Eng-/-}$ mouse
7	$Col1a1^{Eng-/-}$
8	$Col1a1^{Eng+/-}$
9	WT
10	H_2O (Negative control)
11	DNA ladder

B

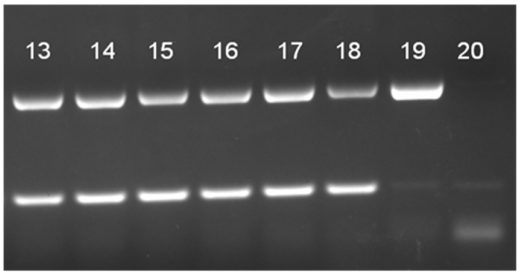

slot	Sample
13	$Col1a1^{Eng-/-}$ mouse
14	$Col1a1^{Eng-/-}$ mouse
15	$Col1a1^{Eng-/-}$ mouse
16	$Col1a1^{Eng-/-}$ mouse
17	$Col1a1^{Eng-/-}$ mouse
18	$Col1a1^{Eng-/-}$
19	$Col1a1^{Eng+/-}$
20	H_2O (Negative control)

Supplementary figure 1: Representative image of the genotyping performed for the presence of endoglin floxed genes (**A**) and for expression of CRE (**B**) for all mice used in the experiments.

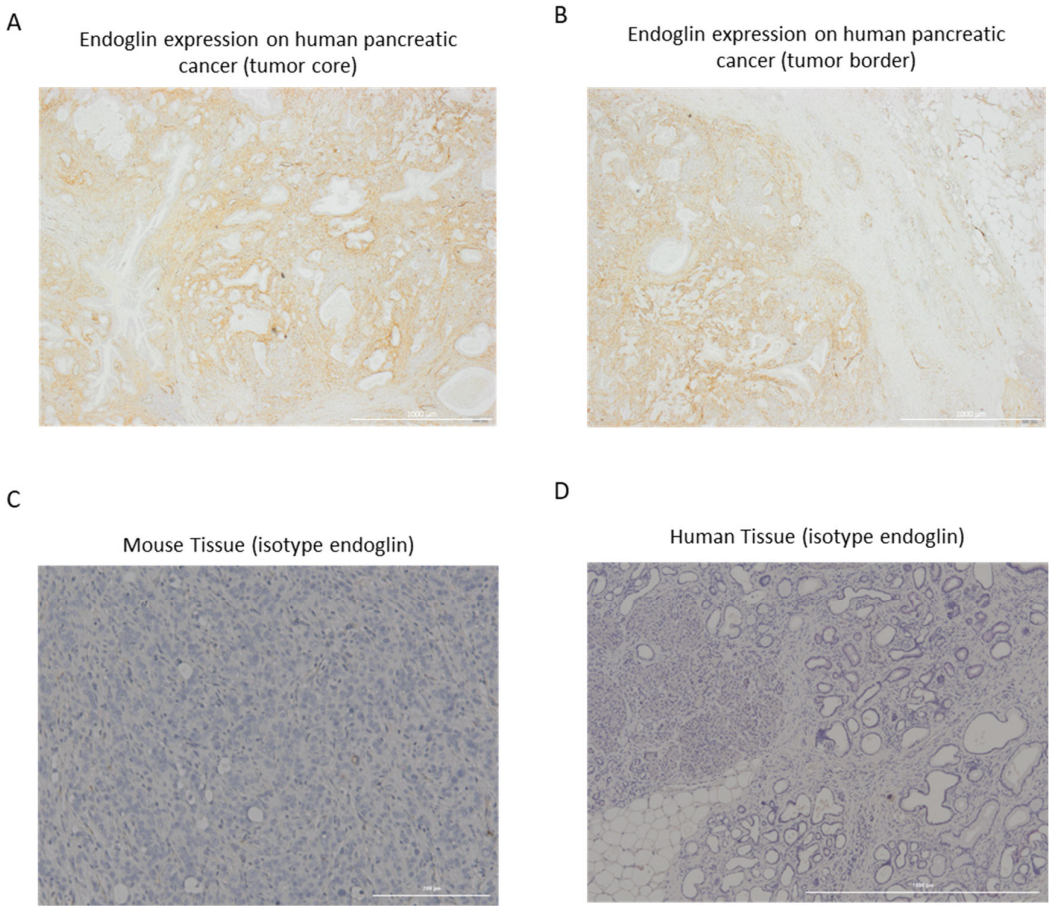

Supplementary figure 2: A Representative image of human endoglin expression on human pancreatic cancer tumor cores (n = 5). **B** Representative image of human endoglin expression on human pancreatic cancer tumor borders (n = 5). **C** Isotype control for endoglin staining on mouse pancreatic cancer tissue. **D** Isotype control for endoglin staining on human pancreatic cancer tissue.

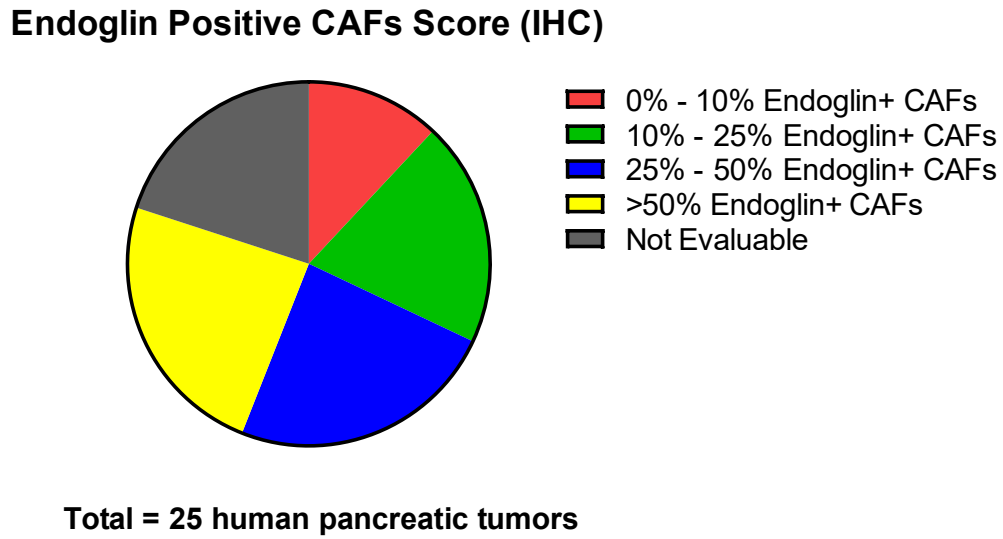

Supplementary figure 3: CAF-specific endoglin expression was scored on a scale of 1 to 4 (1: 0-10%; 2: 10%–25%; 3: 25%–50%, and 4: >50% endoglin positive CAFs vs total amount of CAFs) in a blinded manner by two independent observers.

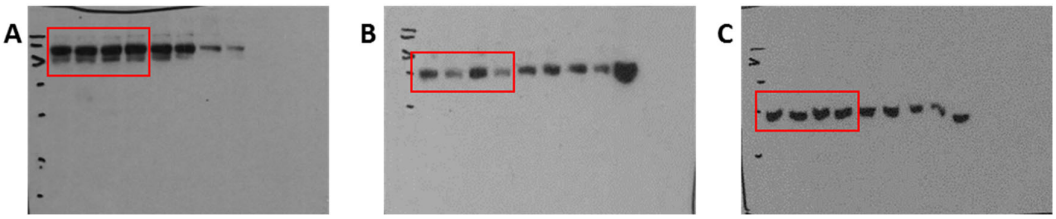

Supplementary figure 4: Full-length blot, the red borders indicate where the blot was cropped. **A** Endoglin protein expression on human pancreatic fibroblasts. **B** Basal and BMP9-induced downstream signaling (pSMAD1) was inhibited with TRC105. **C** Loading control (actin)

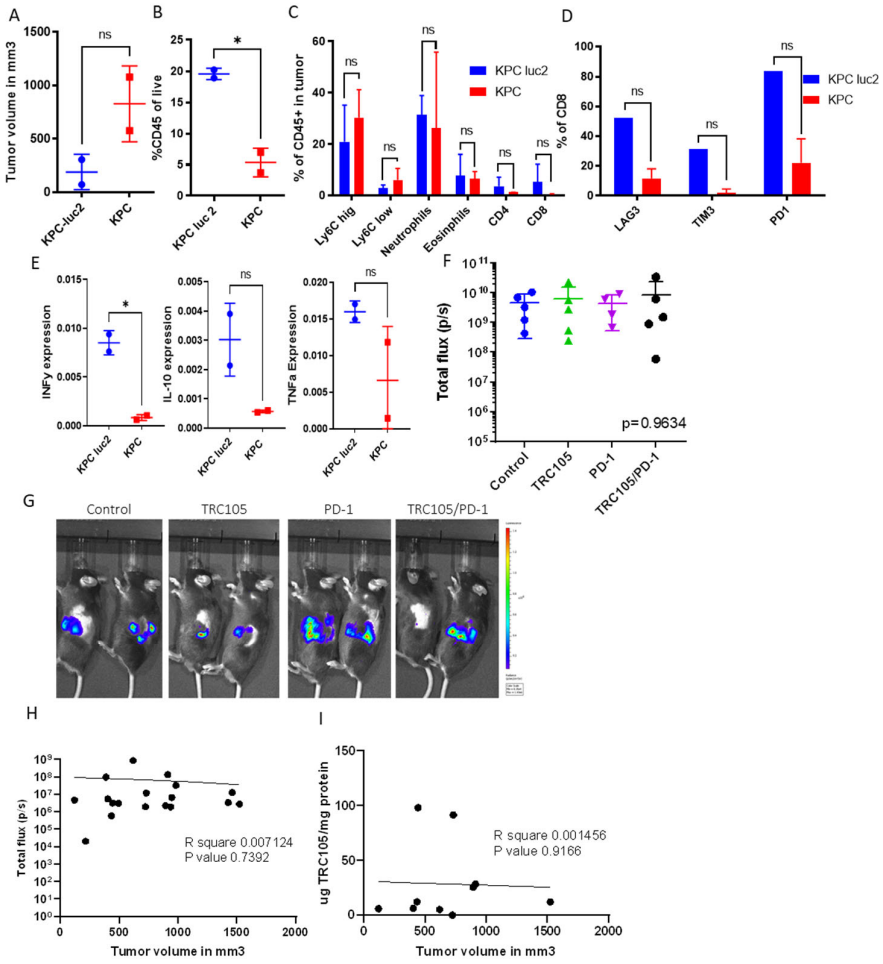

20 **Supplementary figure 5: A** Decreased tumor growth in the KPC-luc2 versus KPC parental cells,
21 accompanied by **B** increased CD45+ cells (n=2 mice per group). **C** Flow cytometry analysis on
22 different immune cell populations **D** Activation markers on CD8+ T-cells in the KPC-3-Luc2
23 versus KPC-3 (n=2 mice per group). **E** cytokine profile of the KPC-Luc2 versus KPC cells (n=2
24 mice per group). **A – E** Student T-test was performed to calculate differences indicated in the
25 graphs *p=<0.05 **p=<0.01. **F** Randomization of pancreatic tumors on bioluminescent signal,
26 (p=0.9634 by ANOVA, n=4-5 mice per group). **G** Representative bioluminescent pictures from
27 mice depicted in figure 3 . **H** No correlation between tumor volume and luciferase signal (n=18
28 mice linear regression was used to calculate the R square and P-value). **I** TRC105 accumulation
29 did not correlate with decreased tumor volume (n=7 mice linear regression was used to
30 calculate the R square and -value). All graphs represent mean +/- SD.

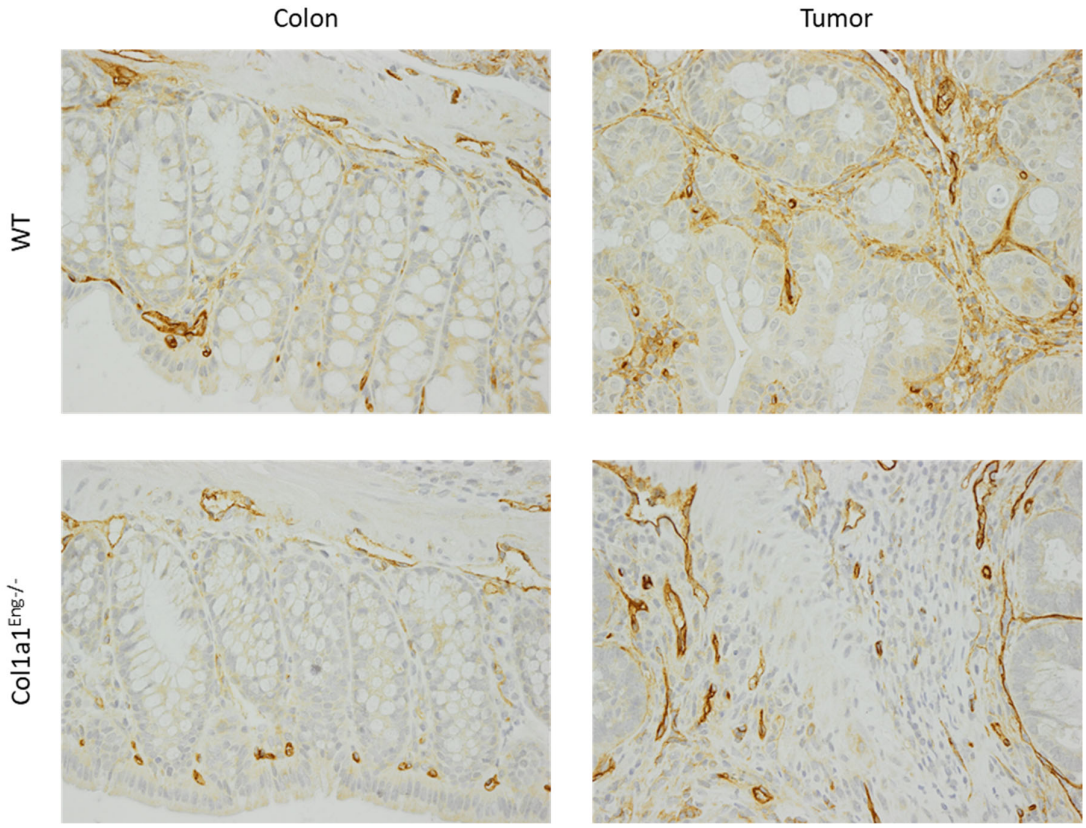

Supplementary figure 6: Images of endoglin expression by wild-type (upper panels) and Col1a1$^{Eng-/-}$ (lower panels) mice in the colon (left panels) and in the colonic adenomas (right panels). The wild-type mice show endoglin expression on endothelial cells as well as fibroblasts. The Col1a1$^{Eng-/-}$ mice only show endoglin expression on endothelial cells.

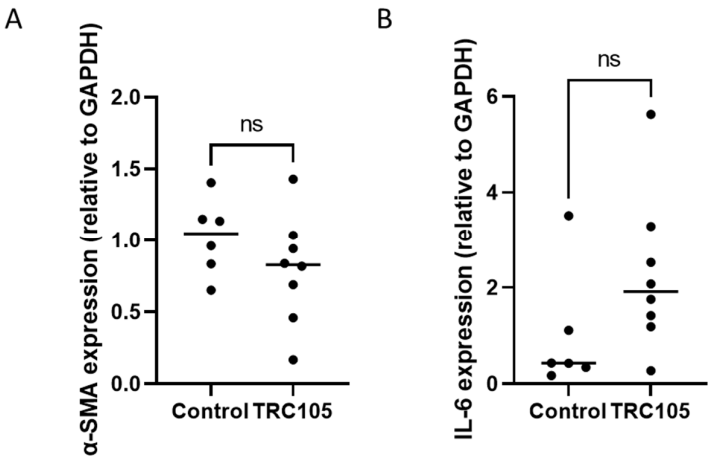

Supplementary figure 7: α-SMA (**A**) and IL-6 (**B**) expression by TRC105 treated mice compared to the control group (n=5-8 mice per group).

Supplementary table 1: Flow cytometry panel

Epitope	Fluorchrome	Manufacturer
CD3	V450	eBioscience
CD4	Qdot605	Biolegend
CD8	Alexa 700	BD Biosciences
CD45.2	APC-Cy7	Thermo Fisher
Nk1.1	PE-Cy7	Biolegend
PD-1	FITCH	Thermo Fisher
TIM3	APC	Thermo Fisher
LAG3	PE	Biolegend
Life death	UV	Thermo Fisher
CD90.2	PE-cy7	Biolegend
CD326 (ep-CAM)	PerCP-Cy5.5	Biolegend
CD45.2	APC-Cy7	Invitrogen
Podoplanin	Alexa Fluor 488	Biolegend
CD31	APC	Invitrogen
Life death	UV	Thermo Fisher

Supplementary table 2: RT-PCR primers

Primer	Forward 5'3' sequence	Reverse 5'3' sequence
αSMA	GTCCCAGACATCAGGGAGTAA	TCGGATACTTCAGCGTCAGGA
CD31	CTCCAACAGAGCCAGCAGTA	GACCACTCCAATGACAACCA
CD45	GAGGTGTCTGATGGTGCAAG	TGTATTCCACTAAAGCCTGATGAA
Endoglin	TGAATGGCAACCACGAGC	GCAGGATGAGAATGGCGTC
Vimentin	TGGCACGTCTTGACCTTGAA	GGTCATCGTGATGCTGAGAA
HGF	AAGAGTGGCATCAAATGCCAG	CTGGATTGCTTGTGAAACACC
TGFβ1	CAACAATTCCTGGCGTTACC	TGCTGTCACAAGAGCAGTGA
TGFβ2	CCGCCCACTTTCTACAGACCC	GCGCTGGGTGGGAGATGTTAA
TGFβ3	GTTTGCAGCATTTGTGATCG	TGCTCTGAGTGCTCCCTATG
VEGF	CACAGCAGATGTGAATGCAG	TTTACACGTCTGCGGATCTT
BMP-9	CACTCCACTGAGATGTGCGT	GCACAGCAAGCAGCCTATTC
FoxP3	CCCAGGAAAGACAGCAACCTT	TTCTCACAACCAGGCCACTTG
Granzyme B	ACTTTCGATCAAGGATCAGCA	ACTGTCAGCTCAACCTCTTGT
IFNγ	GCTTTAACAGCAGGCCAGAC	GGAAGCACCAGGTGTCAAGT
IL-1β	AAGGGGACATTAGGCAGCAC	ATGAAAGACCTCAGTGCGGG
IL-2	CACCCACTTCAAGCTCCACT	AGGTCCATCAACAGCTGCTC
IL-4	AGATGGATGTGCCAAACGTCCTCA	AATATGCGAAGCACCTTGGAAGCC
IL-5	ACCGAGCTCTGTTGACAAG	TCCTCGCCACACTTCTCTTT
IL-6	GTATGAATAACGATGATGCACTTG	ATGGTACTCCAGAAGACCAGAGGA
IL-8	CGGCAATGAAGCTTCTGTAT	CCTTGAAACTCTTTGCCTCA
IL-10	CCAGGGAGATCCTTTGATGA	AACTGGCCACAGTTTTCAGG
IL-12	GATGACATGGTGAAGACGGC	AGGCACAGGGTCATCATCAA
IL-13	TGAGGAGCTGAGCAACATCACACA	TGCGGTTACAGAGGCCATGCAATA
IL-15	GTGACTTTCATCCCAGTTGC	TTCCTTGCAGCCAGATTCTG
TNFα	TAGCCAGGAGGGAGAACAGA	TTTTCTGGAGGCAGATGTGG
hEndoglin	CCGAGAGGTGCTTCTGGTCC	GTGCAGTGGGATTCCCAGG
hβ-actin	GTTGTCGACGACGAGCG	GCACAGAGCCTCGCCTT